Hydraulic Conductivity in Frozen Unsaturated Soil

Kunio Watanabe
Graduate school of Bioresources, Mie University, Japan
Tomomi Wake
Graduate school of Bioresources, Mie University, Japan

Abstract

Freezing experiments of silt and sand columns were carried out, and water and heat flows were observed. To estimate unsaturated hydraulic conductivity of soils, $K(h)$, at above-freezing and subzero temperatures, Darcy's law was solved under a non-isothermal condition with ice formation. $K(h)$ steeply decreased with decreasing soil water pressure, h, and more gradually decreased with soil freezing. The results show that the hydraulic model, in which water content became constant under $h< -10^5$ cm, underestimated the $K(h)$ of frozen soil, and suggest that the impedance factor, which reduced $K(h)$ for frozen soil, is not necessary when accurate soil water and soil freezing characteristics are available. The hydraulic model, which can express two types of soil water flow, such as capillary and film flows, appears to be useful for expressing the hydraulic properties of soils under the freezing process.

Keywords: soil freezing characteristic; soil water characteristic; TDR; unsaturated hydraulic conductivity; water and heat flows.

Introduction

Knowledge of water flow in frozen and thawing ground is important to investigating water and solute redistributions in soil during winter (Baker & Spaans 1997) and in studying the mechanism of frost heaving (Wettlaufer & Worster 2006). Changes in soil properties, such as hydraulic conductivity, have also received research attention. For example, changes caused by ground freezing have been examined by applying an artificial soil-freezing technique to stabilize soil and form a barrier against hazardous waste (McCauley et al. 2002). Moreover, a major concern of hydrological and climate modeling is how to express change in soil hydraulic properties.

Burt & Williams (1976) and Horiguchi & Miller (1983) measured the steep decrease in hydraulic conductivity with soil freezing, although within a small temperature range. Using oil as a fluid, McCauley et al. (2002) measured saturated hydraulic conductivity of frozen soil at various temperatures. However, few experimental studies have examined the unsaturated hydraulic conductivity of frozen soil, $K_f(h)$. The unsaturated hydraulic conductivity of unfrozen soil, $K(h)$, is usually expressed by the formula proposed by Brooks & Corey (1964), Clapp & Hornberger (1979), or van Genuchten (1980). For frozen soil, Harlan (1973) used $K(h)$ instead of $K_f(h)$, assuming the same film-water geometry between frozen and unfrozen soils. However, numerical simulations have suggested that this assumption overestimates water flow near the freezing front (Harlan 1973, Taylor & Luthin 1978, Jame & Norum 1980). Guymon & Luthin (1974) and Tao & Gray (1994) expressed $K_f(h)$ from $K(h)$ by subtracting ice content from saturated water content. When the soil is frozen, the presence of ice in some pores may block water flow. To account for this blocking, several impedance factors have been introduced (James & Norum 1980, Lundin 1990, Smirnova et al. 2000). However, Black & Hardenberg (1991) criticized the use of an impedance factor, stating that it is a potent and wholly arbitrary correction function for determining $K_f(h)$. Newman & Wilson (1997) also concluded that an impedance factor is unnecessary when an accurate soil water characteristic curve and relationship between $K(h)$ and soil water pressure are defined.

Measuring unsaturated hydraulic conductivity for frozen soil remains difficult, and a complete expression for $K_f(h)$ is still not available. In addition, the model for $K_f(h)$ should be correlated with the soil water characteristics and soil freezing characteristics for ease of use in numerical simulations (Watanabe et al. 2007). In this experiment, we estimated $K_f(h)$ from water and heat flow measurements in a frozen soil column and discuss a model for $K_f(h)$.

Theory

Assuming that vapor and ice flows are negligible, variably saturated water flow in above-freezing and subzero soil is described using a modified Richards equation as follows (Noborio et al. 1996, Hansson et al. 2004).

$$\frac{\partial \theta(h)}{\partial t} + \frac{\rho_i}{\rho_l}\frac{\partial \theta_i(T)}{\partial t} = \frac{\partial}{\partial z}\left(K(h)\frac{\partial h}{\partial z} + K(h) + K(h)\gamma h \frac{\partial T}{\partial z} \right) \quad (1)$$

where θ is volumetric liquid water content, θ_i is volumetric ice content, t is time, z is a spatial coordinate, ρ_i is density of ice, ρ_w is density of water, h is the water pressure head, T is temperature, and γ is the surface tension of soil water. The terms in parentheses on the right-hand side of equation (1) represent the water flux, J_w, obtained from the change in the amount of liquid water and ice. Thus, if we measure the pressure and temperature gradient, $K(h)$ [or $K_f(h)$ at subzero temperature] would be derived as

Table 1. Experimental conditions and physical properties of soil.

		FSi	TDS
Bulk density	g cm^{-3}	1.18	1.45
θ when packed	m^{3}m^{-3}	0.40	0.15
θ saturation	m^{3}m^{-3}	0.569	0.36
Thermal conductivity*	W m -		
at θ = 0.00 (frozen)	^{1}K^{-1}	0.20(0.20)	0.25(0.25)
at θ = 0.17 (frozen)			0.96(1.50)
at θ = 0.24 (frozen)			
at θ = 0.29 (frozen)		0.52(0.55)	1.06(1.05)
Saturated hydraulic cond.			50.6
	cm h^{-1}	0.66(0.76)	
		0.25	
van Genuchten parameter			
θ_r	m^{3}m^{-3}	0.03	0.015
α	m^{-1}	0.16	3.36
n		1.38	7
l		0.552	-0.5
Durner parameter			
θ_r	m^{3}m^{-3}	0.06	0
α_1	m^{-1}	0.35	3.466
n_1		3.10	6.40
l		–0.08	-0.5
α_2	m^{-1}	0.011	0.027
n_2		1.70	1.40
w_2		0.461	0.105

*The value for thermal conductivity is average of 2 to 20°C for unfrozen soil and -5 to -20°C for frozen soil.

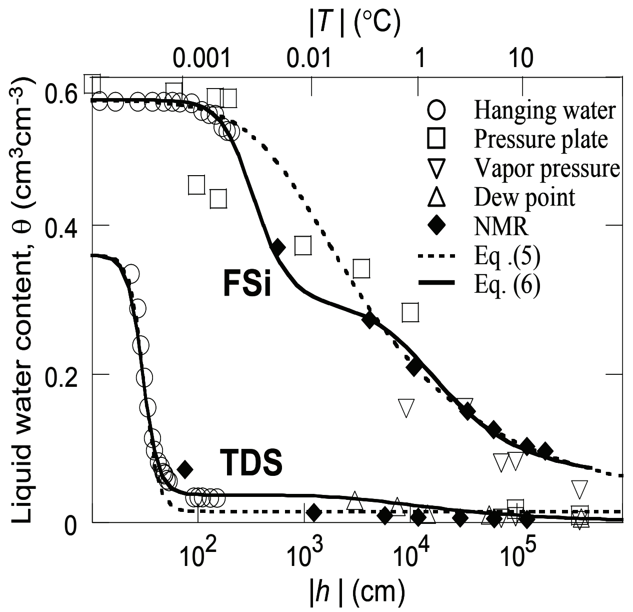

Figure 1. Soil water characteristics measured by hanging water, pressure plate, vapor pressure, and chilled mirror dew point measurement methods, and soil freezing characteristics measured by pulsed NMR measurement for FSi and TDS (in thawing process).

$$K(h) = -\frac{J_w}{\left(\frac{\Delta T}{\Delta z}\gamma h + \frac{\Delta h}{\Delta z} + 1\right)} \tag{2}$$

The value of h in unfrozen soil can be obtained from the soil water characteristics (relationship between θ and h) when measuring the profile of θ, while h in frozen soil can be calculated from the temperature profile derived from the generalized form of the Clausius–Clapeyron equation by assuming a differences between ice and water. Specifically, the ice pressure is sometimes assumed to equal zero gauge pressure (Williams & Smith 1989, Hansson et al. 2004):

$$\frac{dP}{dT} = \frac{L_f}{v_l T} \tag{3}$$

where P is the pressure (= $\rho_w gh$), g is the acceleration due to gravity, L_f is the latent heat of freezing, and v_l is the specific volume of water. Thus, equation (3) gives the soil freezing characteristics (relationship between θ and T) from the soil water characteristics and vice versa.

Material and Methods

The samples used in this study were Fujinomori silt (FSi) and Tottori dune sand (TDS). Figure 1 shows the soil water characteristics measured by several physical methods (Jury & Horton 2004) for both soils as well as soil freezing characteristics measured by pulsed nuclear magnetic resonance (NMR) measurement and depicted by equation (3). FSi is highly susceptible to frost and retains much liquid water even when $|h| > 10^4$ cm ($T < -1$°C), while for TDS, θ = 0.03 when $|h| > 10^2$ cm ($T < -0.01$°C).

The TDS were preliminarily washed in deionized water, and the FSi was passed through a 2 mm screen. Each sample was mixed with distilled and deionized water and packed into an acrylic column with an internal diameter of 7.8 cm and a height of 35 cm. Table 1 lists the experimental conditions and physical properties of the samples. Fifteen copper-constantan thermocouples and seven time domain reflectometry (TDR) probes were inserted into each column, and the side wall of the column was insulated. The TDR was preliminarily calibrated for measuring unfrozen water content by comparison to the pulsed NMR measurement. The column was settled at an ambient temperature of 2°C for 24 h to establish initial water and temperature profiles and then frozen from the upper end by controlling temperature at both ends of the column (T_L = -8°C and T_H = 2°C). During the experiment, no water flux was allowed from either end, and profiles of temperature, water content, and solute concentration (EC_a) were monitored using thermocouples and TDRs. A series of experiments with different durations of freezing were then performed for each freezing condition (i.e., same freezing rate and temperature gradient). At the end of the experimental series, the sample was cut into 2.5 cm intervals to measure the total water content by the dry-oven method. From thermocouples and TDR readings, it was confirmed that each column had the same temperature and water profiles during the series of experiments.

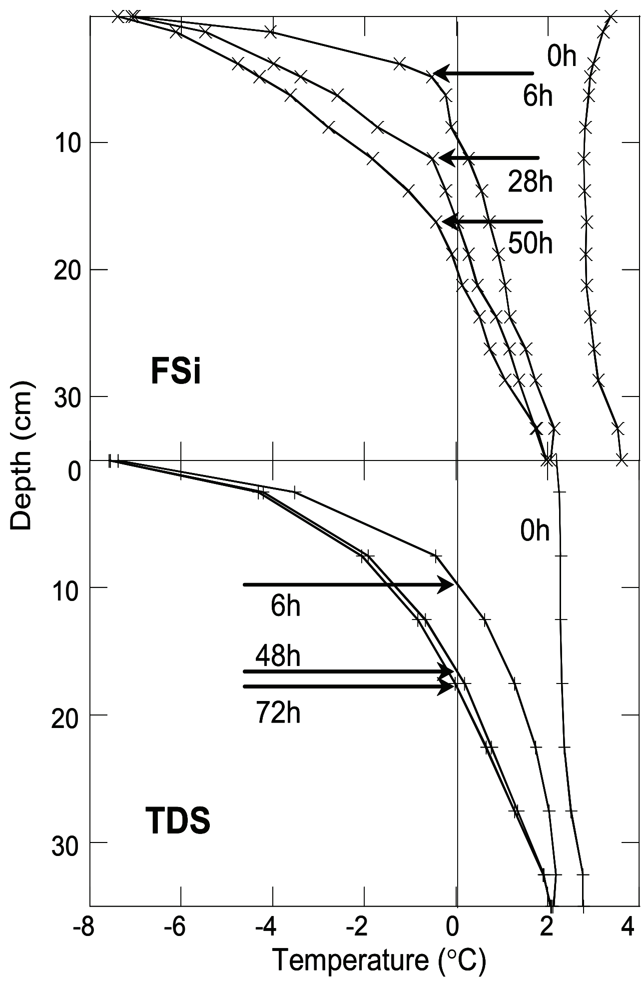

Figure 2. Temperature profiles for FSi (0, 6, 28, 50 h after freezing started) and TDS (0, 6, 48, 72 h after freezing started). Arrows represent the freezing front.

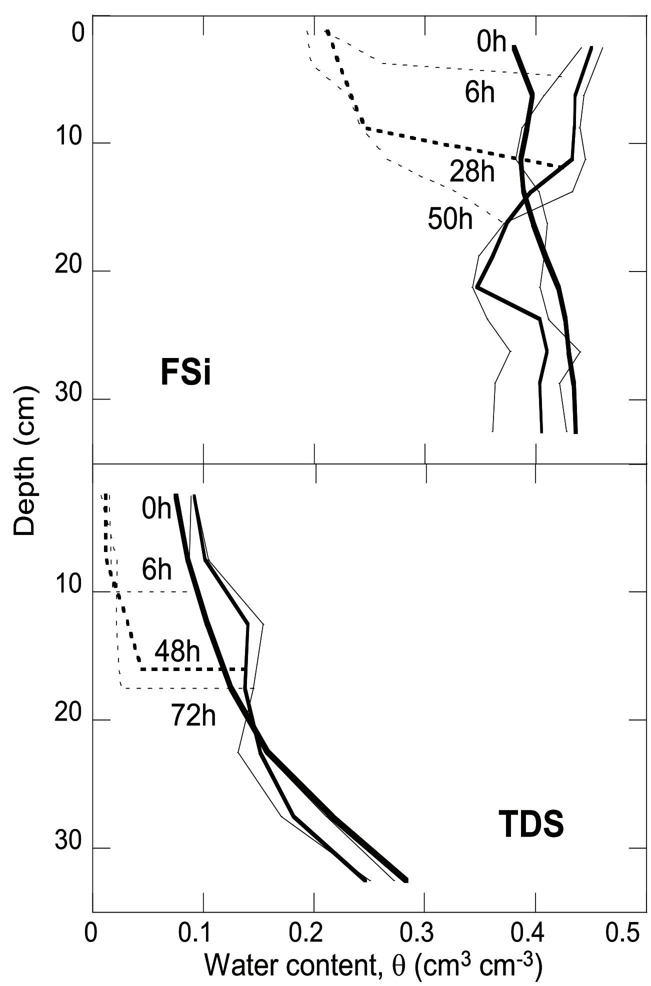

Figure 3. Moisture profiles for FSi and TDS at the same freezing time as shown in Figure 2. The solid line and dashed line represent total water and unfrozen water contents, respectively.

Results

Heat and water flow

Figure 2 shows temperature profiles of the freezing soils. When both ends of the column were set at different temperatures, the soil near the column ends quickly reached the required temperatures. In FSi, the advancing rate of the 0°C isotherm was 1.57, 0.34, and 0.16 cm h^{-1} for 0–6, 6–24, and 24–48 h, respectively, and approximately 0.25°C lowering of the freezing point was observed. The freezing rate of TDS was similar to that of FSi, although TDS had larger thermal conductivity (Table 1). Even after 72 h, the temperature profile of the subzero area in TDS did not reach a linear shape as in FSi and in the unfrozen area in TDS.

Figure 3 presents water profiles in FSi and TDS at the same freezing time as shown in Figure 2. The solid line indicates total water content, θ_t, measured by the dry-oven method, and the dashed line indicates unfrozen water content measured by TDR. The ice content, θ_i, was obtained by subtracting the unfrozen water from the total water content. FSi had a relatively vertical initial θ profile, having similar θ values for h <100 cm (Fig. 1). An increase of θ_t, decrease of θ in the frozen area, and decrease of θ in the unfrozen area with the advancing freezing front were observed, implying that the soil water flowed not only through the unfrozen area, but also the frozen area. The gradient of the initial θ profile of TDS corresponded to its soil water characteristics (Fig. 1). In TDS, the soil water in the unfrozen area flowed to and accumulated near the freezing front because of suction at the freezing front caused by ice formation. Water flow in the unfrozen area continued 48 h or later after freezing began, although there was no apparent advance of the freezing front. Meanwhile, much less water flow was observed in the frozen area.

The profile of water flux, J_w, was then calculated by developing θ profiles (Fig. 3) with the boundary condition of no water flux. In early stage of freezing (0–6 h), soil water in almost the entire column moved upward at about $J_w = 0.04$ cm h^{-1} for FSi and $J_w = 0.01$ cm h^{-1} for TDS. The progression of the peak observed in the J_w profile coincided with the freezing front. In the frozen area, J_w in SFi was ≥10 times larger than that in TDS and exponentially decreased as the temperature decreased ($J_w = 0.007|T|^{-0.69}$ for FSi and $0.0012|T|^{-1.45}$ for TDS).

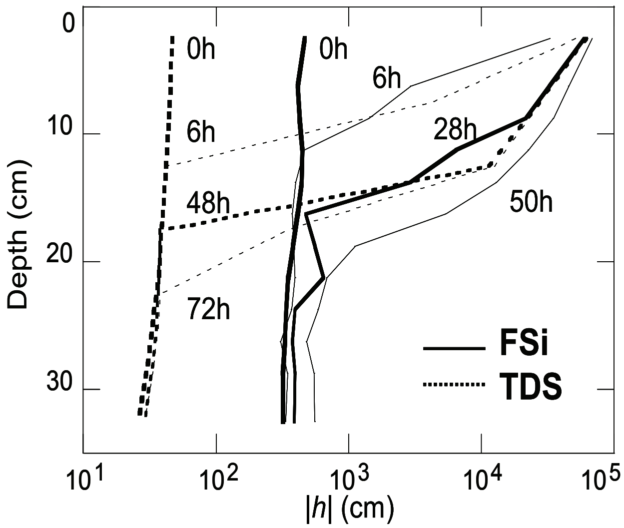

Figure 4. Profile of soil water pressure estimated from Figures 2 and 3.

Change in hydraulic conductivity

Figure 4 shows the profile of soil water pressure h estimated by the soil water characteristics (Fig. 1) with the θ profile (Fig. 3) and equation (3) with the temperature profile (Fig. 2). Solute effect was negligible during the experiments, since very low solute concentration was confirmed by TDR (EC_a) readings. Note that for equation (3) there was discontinuity in the h profiles near 0°C, especially for unsaturated soil; therefore, we used linear interpolation to connect the closest calculated h values between the unfrozen and frozen areas. With freezing, $|h|$ steeply increased ($h < -10^3$ cm). A larger difference in h between unfrozen and frozen areas was observed in TDS than in FSi.

The non-isothermal version of Darcy's law (Eq. 2) could consequently by solved with the J_w, T, and h profiles, obtaining the relationship between the unsaturated hydraulic conductivity, $K(h)$, at above-zero and subzero temperatures with the soil water pressure, as shown in Figure 5. In the range $h > -10^3$ cm (unfrozen), $K(h)$ decreased steeply with increasing $|h|$, while it decreased gradually in the range $h < -10^3$ cm (frozen). Similar $K(h)$ was observed when different freezing conditions were applied (T_L = -5°C and T_H = 5°C in Fig. 5 for TDS). These changes were clearer for $K(h)$ of TDS, which agreed well with the value obtained using the evaporation method (Sakai & Toride 2007). In the frozen area, $K(h)$ in FSi was about 10 times larger than that in TDS, which is why more water flow was observed in frozen FSi. Figure 6 shows the relationship between $K(h)$ and liquid (unfrozen) water content measured by TDR. In frozen TDS, $K(h)$ decreased steeply from 10^{-5}–10^{-8} cm h^{-1} with decreasing θ from 0.04–0.01 cm^3 cm^{-3}, while $K(h)$ of frozen FSi decreased more gradually.

The $K(h)$ of frozen soil also correlated with temperature T and with ice content θ_i. The decrease of $K(h)$ with lowering T and θ_i was well fitted by power law as $K(h) = 3 \times 10^{-6}\,|T|^{-1.49}$ and $K(h) = 2.3 \times 10^{-8}\,\theta_i^{-2.42}$ for FSi, and $K(h) = 0.7 \times 10^{-6}\,|T|^{-1.75}$ and $K(h) = 8.2 \times 10^{-14}\,\theta^{-6.96}$ for TDS. This power law relationship was consistent with the relationship between J_w and $|T|$ mentioned above. The θ_I–T relationship is sometimes expressed by power law (Anderson & Tice 1972) and can be converted through equation (3) to a θ -h relationship, which may also be expressed by power law (Brooks & Corey 1964). The shape of the formula indicating $K(h)$ may arise from the soil water characteristics (θ-h) and soil freezing characteristics (θ_i-T).

Discussion

Soil freezing characteristics

Soil freezing characteristics are sometimes interpreted from the surface force, pore curvature, when solute effect is negligible (Dash et al. 1995, Watanabe & Mizoguchi, 2002). The surface force accounts for the power law shape of soil freezing characteristics and the effect of the curvature known as the Gibbs–Thomson effect, which creates a shoulder to the soil freezing characteristics by means of the freezing temperature depression, $T_m - T$ depending on the soil pore radius r:

$$T_m - T = \frac{T_m \sigma}{\rho_i L_f r} \tag{4}$$

where T_m is the freezing temperature of bulk water and σ is the ice-water interface free energy. In the soil pore size distribution, two peaks are presumed: one from pores among the soil particles (r = 5–50 μm) and the other from pores on the particle surface (r = 3–10 nm). These peaks would yield two shoulders to the soil freezing characteristics around -0.001 to -0.1°C and -2.5 to -10°C, respectively. By converting the soil freezing characteristics to soil water characteristics through equation (3), the warmer shoulder would correspond to air entry. In the range from water saturation to the other (colder) shoulder, soil water will flow predominantly as capillary flow, but will change to film flow at h lower than the colder shoulder. Soil water characteristic models proposed by Brooks & Corey (1964) and van Genuchten (1980) (Eq. 5) are intended to express unsaturated soil with moderate h and give the constant θ (defined as resident water content, θ_r) at extremely low h. These models, therefore, cannot express the area around the colder shoulder, which is an important portion for soil freezing characteristics (Fig. 1). Durner (1994) combined two van Genuchten models, which express different soil water characteristics, to describe water retention in a soil having a dual porosity distribution (Eq. 6):

$$S_e = \left(1 + |\alpha h|^n\right)^{-m} \tag{5}$$

$$S_e = w_1\left[1 + (\alpha_1 h)^{n_1}\right]^{-m_1} + w_2\left[1 + (\alpha_2 h)^{n_2}\right]^{-m_2} \tag{6}$$

where $S_e = (\theta - \theta_r)(\theta_s - \theta_r)^{-1}$, $m = 1 - n^{-1}$, $w_1 = 1 - w_2$, θ_s is saturated water content, α and n are empirical parameters,

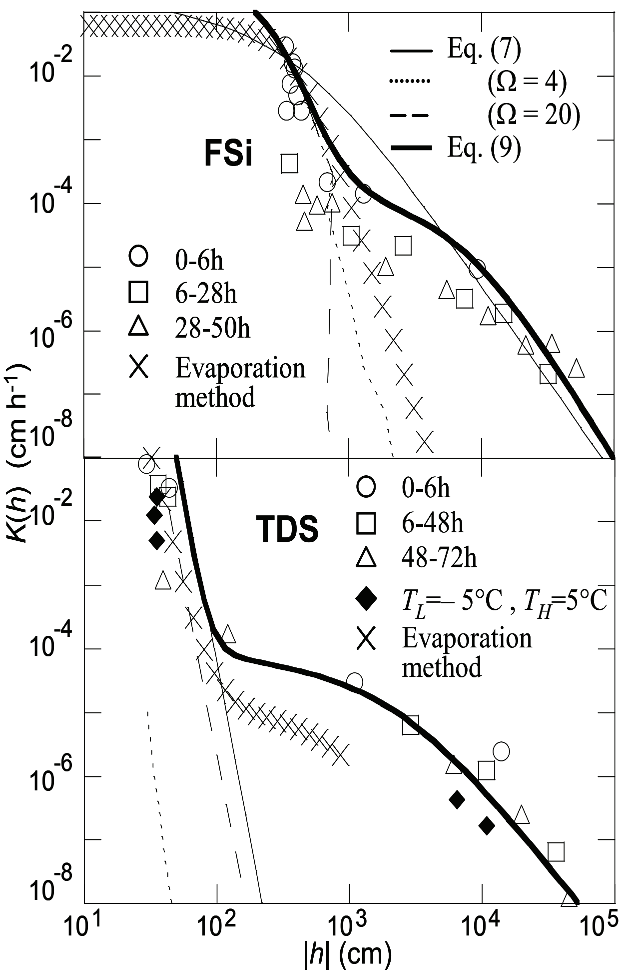

Figure 5. Relationship between unsaturated hydraulic conductivity [$K(h)$] and soil water pressure at above-zero and subzero temperature. Table 1 lists the parameters for equations (7) and (9).

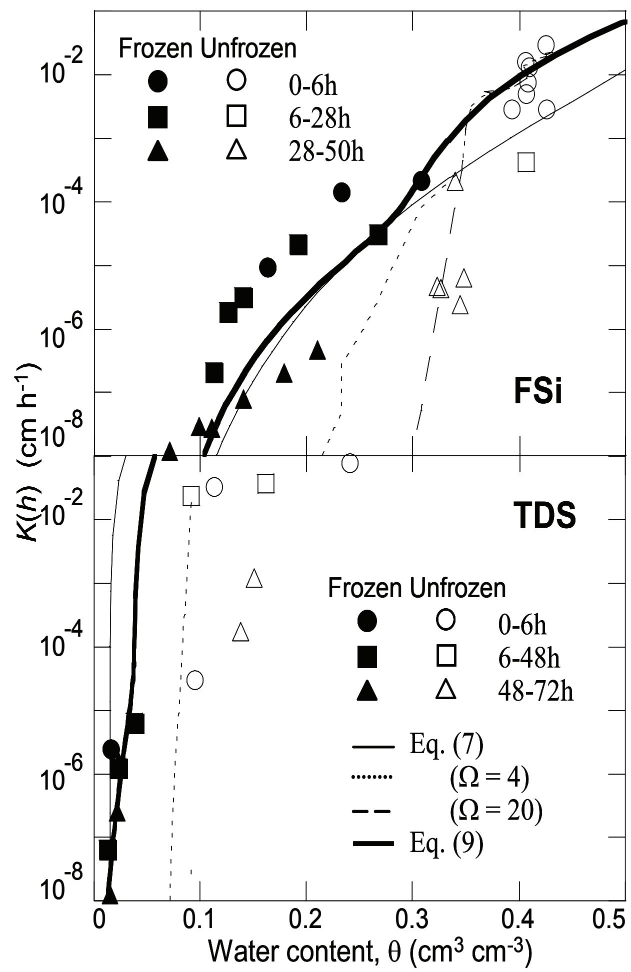

Figure 6. Relationship between unsaturated hydraulic conductivity, $K(h)$, and soil water content at above-zero and subzero temperature. Table 1 lists the parameters for equations (7) and (9).

and w_2 is the weighting factor. Using the parameters listed in Table 1, equation (6) was well fitted to a wide range of soil water characteristics, including soil freezing characteristics, for FSi and TDS (Fig. 1).

Unsaturated hydraulic conductivity for frozen soils

The unsaturated hydraulic conductivity for unfrozen soil, $K(h)$, is often derived from equation (5) (van Genuchten 1980) as follows:

$$K(h) = K_s S_e^l \left[1-\left(1-S_e^{1/m}\right)^m\right]^2 \tag{7}$$

where l is the pore-connectivity coefficient. For frozen soil, $K(h)$ is sometimes reduced by an impedance factor Ω (Lundin 1990, Hansson et al. 2004):

$$K(h)_{frozen} = 10^{-\Omega\theta_i/(\theta_t-\theta_r)} K(h) \tag{8}$$

Applying equations (7) and (8) to our measured $K(h)$ verified that equation (7) could not fit the gradient change of $K(h)$ around $h = 10^{-3}$ cm for FSi and underestimated $K(h)$ at $h < -10^2$ cm for TDS (Fig. 5). The impedance factor might be useful for expressing the steep decrease of $K(h)$ near 0°C, if equation (5) were fitted to the whole range of soil water characteristics (FSi in Figs. 5, 6). However, use of an impedance factor requires caution since it will underestimate $K(h)$ as freezing progresses.

The design of equation (7) was based on the bundle of capillary tube model in which water flow decreases with square decrease in the pore (tube) radius, as Poiseuille flow, and produces a linear reduction in $K(h)$ on a log–log scale when θ is constant. On the other hand, film water can be regarded as the flow proportional to the first or less root of film thickness. The $K(h)$ of frozen soil consequently has a lower grade than that of unfrozen soil. Thus, the Durner model was again applied to $K(h)$, taking care that θ did not become constant at $10^{-3} < h < 10^{-6}$ cm ($-0.1 < T < -100$°C).

$$K(S_e) = K_s\left(w_1 S_{e1} + w_2 S_{e2}\right)^l \times \frac{\left(w_1\alpha_1\left[1-\left(1-S_{e1}^{1/m_1}\right)^{m_1}\right] + w_2\alpha_2\left[1-\left(1-S_{e2}^{1/m_2}\right)^{m_2}\right]\right)^2}{\left(w_1\alpha_1 + w_2\alpha_2\right)^2} \tag{9}$$

Equation (9) showed good agreement with the $K(h)$ obtained from the column freezing experiment (Figs. 5, 6). This model was originally used for explaining water flow containing two different flow rates, such as among and within soil aggregates. Our results suggest that this model is also suitable for soils under freezing-thawing processes, in which soil water flow changes from capillary flow to film flow.

Conclusion

The sand and silt columns were frozen directionally, and the water and heat flows during soil freezing were measured. The flows depended on the soil types. Unsaturated hydraulic conductivity for frozen and unfrozen soils was estimated by solving Darcy's law under non-isothermal conditions with ice formation, although further consideration of the precision of flux measurements and limits of the Clausius-Clapeyron equation may be required. Hydraulic conductivity steeply decreased with decreasing soil water pressure and water content in unfrozen soil but more gradually decreased in frozen soil. In both unfrozen and frozen states, the silt had higher hydraulic conductivity than the sand, resulting in more water flow during silt freezing.

The shapes of soil water characteristics and soil freezing characteristics were discussed from the viewpoint of the pore size distribution. Use of an impedance factor for calibrating the hydraulic conductivity of frozen soil, which has sometimes created unstable numerical simulations, appears to be unnecessary when the hydraulic model can appropriately express both the soil water and freezing characteristics. Rather, the results suggest that the Durner model is useful for expressing the hydraulic properties affected by the change in the type of water flow during soil freezing.

References

Anderson, D.M. & Tice, A.R. 1972. Predicting unfrozen water content in frozen soils from surface area measurements. *Highway Res. Record*, 393: 12-18.

Baker, J.M. & Spaans, E.J.A. 1997. Mechanics of meltwater movement above and within frozen soil. *Proceedings of International Symposium on Physics, Chemistry, and Ecology of Seasonally Frozen Soils. U.S. Army CRREL Special Report* 97-10, 31-36.

Black, P.B. & Hardenberg, M.J. 1991. Historical perspectives in frost heave research, the early works of S. Taber and G. Beskow. *CRREL Special Report*, 91-23.

Brooks, R.H. & Corey, A.T. 1964. Hydraulic properties of porous media. *Hydrol. Paper 3*. Colorado State Univ., Fort Collins, CO, USA.

Burt, T.P. & Williams, P.J. 1976. Hydraulic conductivity in frozen soils. *Earth Surface Processes* 1: 349-360.

Clapp, R.B. & Hornberger, G.M. 1979. Empirical equations for some soil hydraulic properties. *Water Resour. Res.* 14: 601–604.

Dash, J.G., Fu, H. & Wettlaufer. J.S. 1995. The premelting of ice and its environmental consequences. *Rep. Prog. Phys.* 58: 115-167.

Durner, W. 1994. Hydraulic conductivity estimation for soils with heterogeneous pore structure. *Water Resour. Res.* 30(2): 211-223.

Guymon, G.L., Berg, R.L. & Hromadka, T.V. 1993. Mathematical model of frost heave and thaw settlement in pavement. *CRREL Report* 93-2.

Hansson, K., Šimůnek, J., Mizoguchi, M., Lundin, L.C. & van Genuchten, M.Th. 2004. Water flow and heat transport in frozen soil: Numerical solution and freeze-thaw applications. *Vadose Zone Journal* 3: 693-704.

Harlan, R.L. 1973. Analysis of coupled heat-fluid transport in partially frozen soil. *Water Resour. Res.* 9: 1314-1323.

Horiguchi, K & Miller, R.D. 1983. Hydraulic conductivity of frozen earth materials. *Proceedings of the Fourth International Conference on Permafrost*, Fairbanks, 504-509.

Jame, Y.W. & Norum, D.I. 1980. Heat and mass transfer in freezing unsaturated porous media. *Water Resour. Res.* 16: 811-819.

Jury, A.W. & Horton, R. 2004. *Soil Physics*, Hoboken: John Willey & Sons Inc., 384 pp.

Lundin, L.-C. 1990. Hydraulic properties in an operational model of frozen soil. *J. Hydrol.* 118: 289-310

McCauley, C.A., White, D.M., Lilly, M.R. & Nyman, D.M 2002. A comparison of hydraulic conductivities, permeabilities and infiltration rates in frozen and unfrozen soils. *Cold Regions Sci. Tech.* 34: 117-125.

Newman, G.P. & Wilson, G.W. 2004. Heat and mass transfer in unsaturated soils during freezing. *Can. Geotech. J.* 34: 63-70.

Noborio, K., McInners, K.J. & Heilman, J.L. 1996. Two-dimensional model for water, heat and solute transport in furrow-irrigated soil: I. Theory. *Soil Sci. Soc. Am. J.* 60: 1001-1009.

Sakai, M & Toride, N. 2007. Optimum conditions for predicting unsaturated hydraulic properties using the evaporation method. *J. Jpn. Soc. Soil Phys*. 106: 33-46.

Smirnova, T.G., Brown, J.M., Benjamin, S.G. & Kim, D. 2000. Parameterization of cold-season processes in the MAPS land-surface scheme. *J. Geophys. Res.* 105: 4077-4086.

Tao, Y.X. & Gray, D.M. 1994. Prediction of snowmelt infiltration into frozen soils. *Numerical Heat Transfer, Part A: Applications* 26: 643-665.

Taylor, G.S. & Luthin, J.N. 1978. A model for coupled heat and moisture transfer during soil freezing. *Can. Geotech. J.* 15: 548-555.

van Genuchten, M.Th. 1980. A closed-form equation for predicting the hydraulic conductivity of unsaturated soils. *Soil Soc. Am. J.* 44: 892-898.

Watanabe, K. & Mizoguchi, M. 2002. Amount of unfrozen water in frozen porous media saturated with solution. *Cold Reg. Sci. Tech.* 34: 103-110.

Watanabe, K. Toride, N., Sakai, M. & Šimůnek, J. 2007. Numerical modeling of water, heat and solute transport during soil freezing. *J. Jpn. Soc. Soil Phys.* 106: 21-32.

Wettlaufer, J.S. & Worster, M.G. 2006. Premelting dynamics. *Annu. Rev. Fluid. Mech.* 38: 427-452.

Williams, P.J. & Smith, M.W. 1989. *The Frozen Earth: Fundamentals of Geocryology*. Cambridge: Cambridge University Press, 360 pp.